ACS APPLIED POLYMER MATERIALS

Letter

Cite This: ACS Appl. Polym. Mater. 2019, 1, 309−314

pubs.acs.org/acsapm

Thiol−Ene Click Post-Polymerization Modification of a Fluorescent Conjugated Polymer for Parts-per-Billion Pyrophosphate Detection in Seawater

Abagail K. Williams,[†] Joshua Tropp,[†] Erin R. Crater, Naresh Eedugurala, and Jason D. Azoulay*

School of Polymer Science and Engineering, The University of Southern Mississippi, 118 College Drive No. 5050, Hattiesburg, Mississippi 39406, United States

Supporting Information

ABSTRACT: The evolution of conjugated polyelectrolytes (CPEs) that transduce analyte−receptor interactions into detectable fluorescent responses in complex aqueous environments is predicated on advancements in molecular design and improved synthetic accessibility. Here, we demonstrate a simple post-polymerization modification protocol, based on thiol−ene click chemistry, that results in the rapid installation of sodium sulfate terminated side-chains to a poly(fluorene-*co*-ethynyl) scaffold. The fluorescence of the resulting water-soluble CPE is quenched by Fe^{3+}, dequenched selectively by pyrophosphate (PPi), and accurately quantifies PPi within ±6 nM in artificial seawater. The broad utility of thiol−ene click chemistry should offer the straightforward integration of diverse sensing elements.

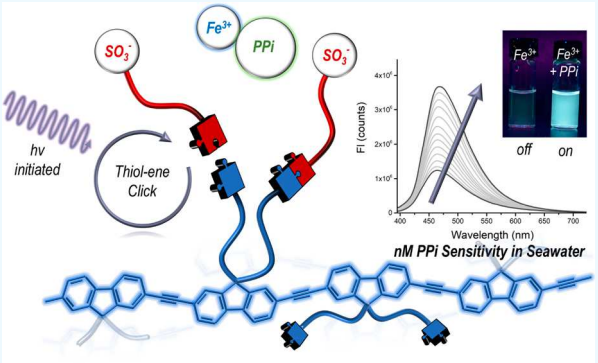

KEYWORDS: *conjugated polyelectrolyte, click reaction, post-polymerization modification, chemical sensing, inorganic phosphate detection, water quality monitoring*

Phosphorus oxyanion detection in complex aqueous environments remains a significant technological challenge requiring the development of straightforward, sensitive, and selective sensing approaches.[1] Pyrophosphate (PPi; $P_2O_7^{4-}$), for example, is ubiquitous in biological systems with roles in cellular energy transduction, biomacromolecule synthesis, extracellular signal mediation, etc.[2−4] The use of PPi as a critical nutrient for enhancing crop yields results in nutrient rich agricultural runoff, which leads to the eutrophication of aquatic ecosystems, growth of algal blooms related to hypoxia and "dead zones", and deposition of toxins in municipal water supplies, thereby negatively impacting human health and the economy.[5,6] There remains a critical need for simple, robust phosphate sensors that reduce the high cost and complexity of collecting data and that better capture intricacies associated with how phosphates exist in biological processes and within ecosystems.

For these reasons, new chemistries for detecting and quantifying phosphates have been at the forefront of research efforts. Small-molecule optical assays predicated on indicator displacement,[1,7] photoinduced electron transfer,[4,8] and monomer−excimer formation[9,10] have been used for PPi detection but are generally limited by ratiometric quenching, narrow selectivity, multistep synthetic approaches, and micromolar sensitivity. Additionally, several supramolecular hosts for phosphorus oxyanions have been developed, but selective binding in water remains a challenge due to competitive solvation.[11,12] These failings have made the transduction of small-molecule binding events into signals with the required sensitivity for biological, physical, and environmental applications a challenge.

Fluorescent conjugated polymers (CPs) and conjugated polyelectrolytes (CPEs) can simultaneously function as molecular recognition and signal transduction elements for anion detection and display unique signal amplification when compared with small molecules, leading to improvements in sensitivity by orders of magnitude.[13,14] Unlike small-molecule systems, CPs transduce signals through exciton migration and are relatively immune to electrostatic and dielectric variations, allowing their successful implementation for sensing applications within complex aqueous environments.[14] Binding events along the polymer capture the diffusing exciton resulting in the collective response of each repeat unit within the exciton diffusion length.[15] The exciton diffusion process and correlated optical response are closely related to the electronic and structural conformation of the polymer backbone, which can be synthetically tuned to incorporate molecular design features that enhance intra- and intermolecular exciton delocalization, leading to stronger amplified signals and detectivity at nanomolar concentrations.[16,17]

Received: November 2, 2018
Accepted: February 1, 2019
Published: February 1, 2019

DOI: 10.1021/acsapm.8b00064
ACS Appl. Polym. Mater. 2019, 1, 309−314

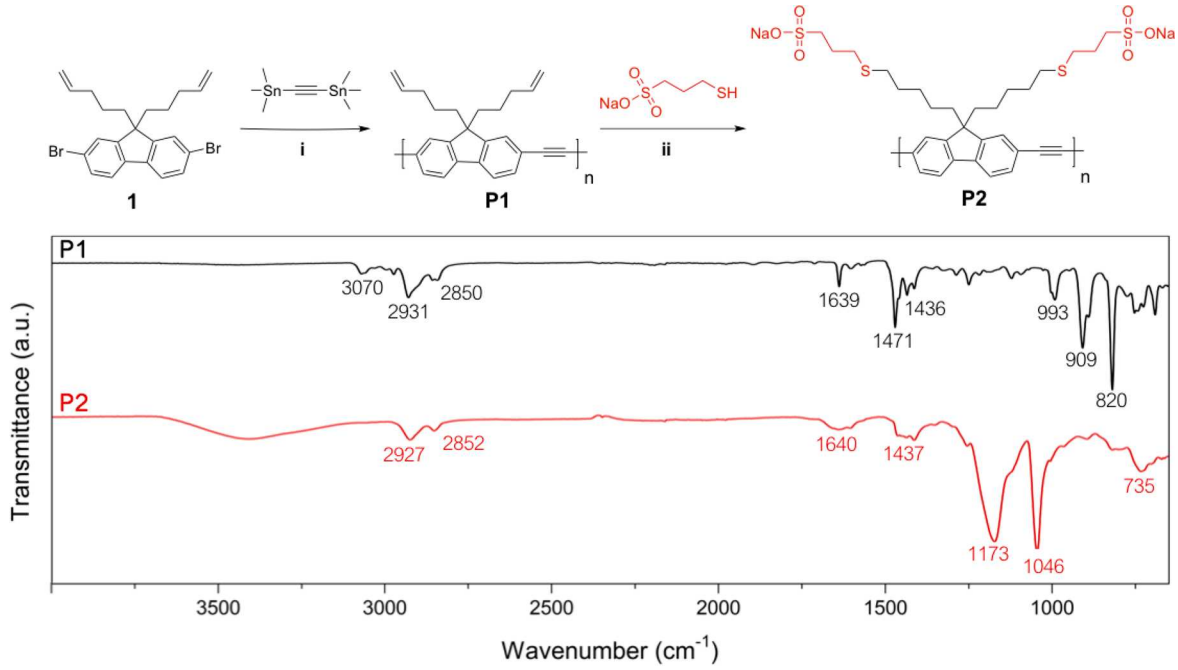

Figure 1. (Top) Synthesis of **P2**: (i) $Pd(PPh_3)_4$ (5 mol %), xylenes/DMF (15:1), 200 mW, 125 °C, 10 min and (ii) Irgacure 819 (2 wt %), tetrahydrofuran/methanol/water, UV, 2 h. (Bottom) Fourier-transform infrared spectra of **P1** and **P2** that highlights the disappearance of alkene groups and appearance of sulfonate groups following the thiol−ene click post-polymerization modification reaction.

This hallmark signal amplification, coupled with the ability to tailor the optical response to various analytes with a diverse set of compatible receptor chemistries, has enabled the development of selective and sensitive CP-based sensors.[18] CPE-based chemosensors have been reported for the selective detection of PPi in aqueous media, such as an on−off−on fluorescent assay based on a sulfonate functionalized poly(fluorene-*co*-phenylene) copolymer.[19,20] This assay incorporates the strong selectivity of molecular recognition elements, high sensitivity from CP signal amplification, and low signal-to-noise ratio characteristic of a "turn-on" output process. Many applications, however, require additional orders of magnitude improvements in sensitivity, more elaborate control over chemical structure, and the eventual integration of more complex recognition elements.

Arduous multistep synthetic procedures, scalability, and a detailed understanding of structure−function−property relationships remain a limiting factor in the development of CPE-based materials and sensors.[13,21] This motivated our investigation of molecular design strategies that afford facile and rapid access to diverse CPEs applied in the context of current sensing platforms.[22−24] Our molecular design begins with poly[2,7-(9,9-di(pent-4-en-1-yl)fluorene)-*alt*-ethynyl] (**P1**), which incorporates pendant pentene substituents at the fluorene bridgehead that provide sufficient solubility of the polymer in organic solvents and allow subsequent functionalization using thiol−ene click chemistry.[25,26] Integration of the ethynyl structural units into poly[2,7-(9,9-di(pentyl-5-(3-sulfopropyl)thio)fluorene)-*alt*-ethynyl] (**P2**) was hypothesized to improve assay sensitivity through enhanced backbone rigidity and planarity, which leads to extension of the exciton diffusion length and increases in the intrinsic tendency of the CPE to aggregate in water.[27]

The synthesis of **P2** was achieved through a microwave-mediated polymerization and subsequent thiol−ene click chemistry post-polymerization modification approach (Figure 1, top). A Stille cross-coupling copolymerization of bis(trimethylstannyl)acetylene with 2,7-dibromo-9,9-di(pent-4-en-1-yl)fluorene (**1**) was carried out via a microwave-assisted reaction using $Pd(PPh_3)_4$ (5 mol %) as the catalyst in xylenes/DMF (15:1) at 125 °C.[28] This approach resulted in the rapid formation of **P1** in a reaction time of 10 min and yield >70% after purification by Soxhlet extraction. Gel permeation chromatography (GPC) at 160 °C in 1,2,4-trichlorobenzene showed a number-average molecular weight, M_n = 6.4 kDa, and dispersity, $Đ$ = 2.3. **P1**, commercially available 3-mercapto-1-propanesulfonic acid sodium salt (∼7.5 equiv), and Irgacure 819 (2 wt %) were suspended in a solvent combination of tetrahydrofuran/methanol/water in a 5:2:2 ratio and subjected to UV irradiation (Rayonet RPR-100, 254 nm, 2.85 mW/cm^2) for 2 h. The polymer was purified by removal of the solvent, precipitation in acetone, and dialysis against water to afford **P2** in 92% yield. The Fourier-transform infrared (FTIR) spectrum of **P1** and **P2** are shown in Figure 1. **P1** has peaks at 909, 993, and 1471 cm^{-1}, corresponding to out-of-plane bending and in-plane scissoring modes of the terminal =C−H groups. Following the thiol−ene click post-polymerization modification these peaks disappear, and new peaks arise at 1173 and 1046 cm^{-1}, characteristic of the S=O stretching vibrations of sulfonate salts. While alkyne stretching modes typically appear between 2100 and 2200 cm^{-1}, there are no peaks present in this region due to the weak vibrational dipole moment of internal alkynes. The complete conversion of terminal olefins by thiol−ene chemistry was also observed via nuclear magnetic resonance (NMR) spectroscopy through the disappearance of peaks between 4.8−5.8 ppm (Figures S1 and S2). This approach afforded the desired CPE in less than a day, circumvented the use of harsh reagents such as sulfuric acid previously used to install sulfonate functionalities, and precluded other arduous multistep synthetic and purification techniques associated with CPE synthesis and isolation.[13,20]

DOI: 10.1021/acsapm.8b00064
ACS Appl. Polym. Mater. 2019, 1, 309−314

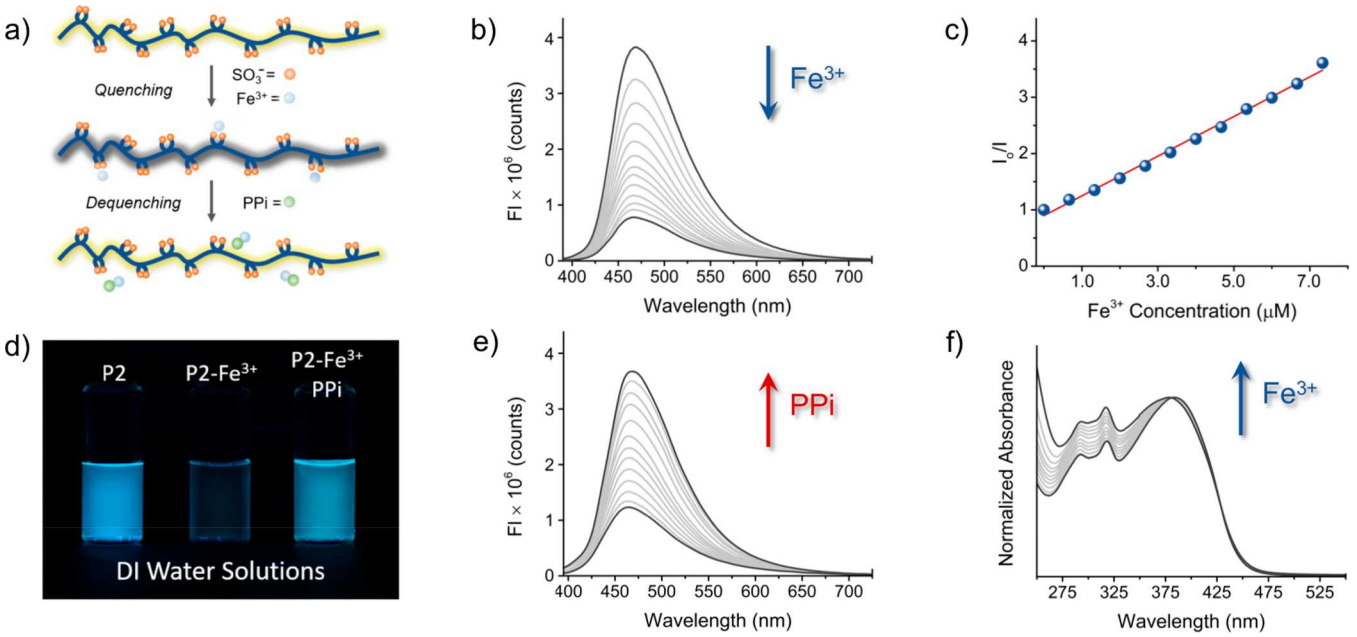

Figure 2. (a) Scheme depicting the fluorescence quenching and dequenching behavior of **P2** upon the addition of Fe^{3+} and PPi, respectively. (b) Fluorescence quenching behavior of an aqueous solution of **P2** (2×10^{-5} M) upon addition of Fe^{3+} (up to 1.3×10^{-5} M) (λ_{ex} = 380 nm). (c) Stern–Volmer plot showing the quenching behavior of **P2** as a function of Fe^{3+} concentration (λ_{ex} = 380 nm, λ_{em} = 463 nm). The K_{sv} value is determined from the slope of the line of best fit. (d) Picture of **P2** solutions in deionized (DI) water showing the on–off–on fluorescence behavior upon subsequent additions of Fe^{3+} and PPi. (e) Fluorescence dequenching of **P2**-Fe^{3+} upon the addition of PPi (up to 5.3×10^{-6} M) (λ_{ex} = 380 nm). (f) The evolution in the absorbance of **P2** (2×10^{-5} M) upon the addition of Fe^{3+} in water.

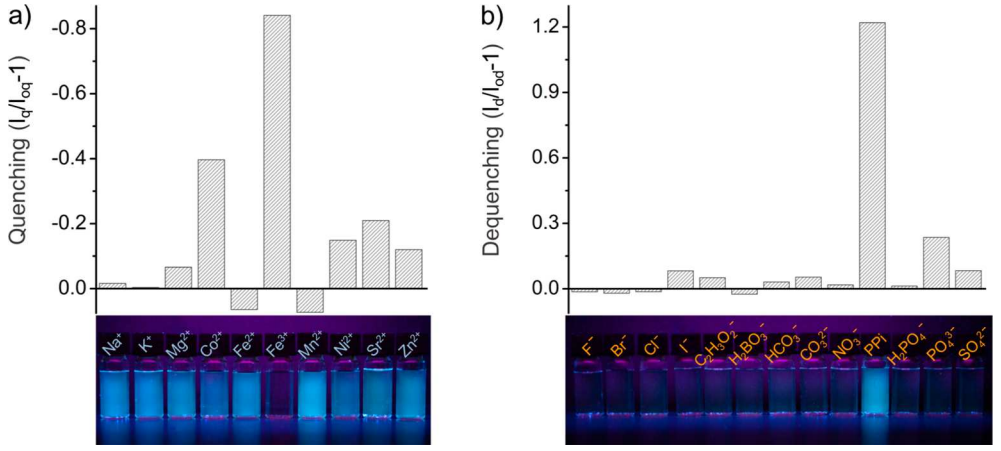

Figure 3. Bar graph summarizing the effect of (a) cations on the fluorescence intensity of **P2** and (b) anions on the fluorescence intensity of **P2**-Fe^{3+} (λ_{ex} = 380 nm, λ_{em} = 463 nm). The initial fluorescence intensities, I_{oq} and I_{od}, are defined as the emission intensity of neat **P2** and **P2** following the addition of Fe^{3+} to quench the fluorescence by 85%, respectively, and I_q and I_d are the fluorescent intensities of **P2** and **P2**-Fe^{3+} in the presence of the various cations and anions, respectively. Negative values correspond to fluorescence quenching, whereas positive values indicate fluorescence dequenching. Pictures showing the fluorescent responses of **P2** and **P2**-Fe^{3+} solutions under UV irradiation (λ_{ex} = 365 nm), in the presence of cations and anions, respectively, are also included.

The pH and photostability of **P2** were investigated using UV–vis and fluorescence spectroscopy (Figures S3 and S4, respectively). The polymer showed high stability in neutral and basic solutions spanning the range associated with marine environments. Consistent with reports of other fluorescent CPs, there was a slow decrease in emission intensity under constant irradiation (see the Supporting Information for full details).[29] The fluorescence quenching and dequenching behavior of **P2** in aqueous solutions was then evaluated through a series of titrations using Fe^{3+} and PPi, respectively (Figure 2). For all optical characterization and assay experiments, the concentration of **P2** is based on the molarity of polymer repeat units in which the polymer repeat unit extinction coefficient was measured to be 9200 L mol^{-1} cm^{-1} (Figure S5). Upon excitation at 380 nm, **P2** exhibits a strong emission between 400 and 700 nm, with maximum intensity centered at 463 nm. Upon titration with Fe^{3+}, the fluorescence of **P2** was strongly quenched with maximum quenching, defined as the point at which the fluorescence intensity does not decrease upon further addition of Fe^{3+} to the **P2** solution, observed at 1.3×10^{-5} M Fe^{3+} (Figure 2b). A Stern–Volmer plot was obtained by plotting I_o/I against the Fe^{3+} concentration, where I_o and I are the fluorescence intensities of **P2** in the absence and presence of Fe^{3+}, respectively, and the

DOI: 10.1021/acsapm.8b00064
ACS Appl. Polym. Mater. 2019, 1, 309–314

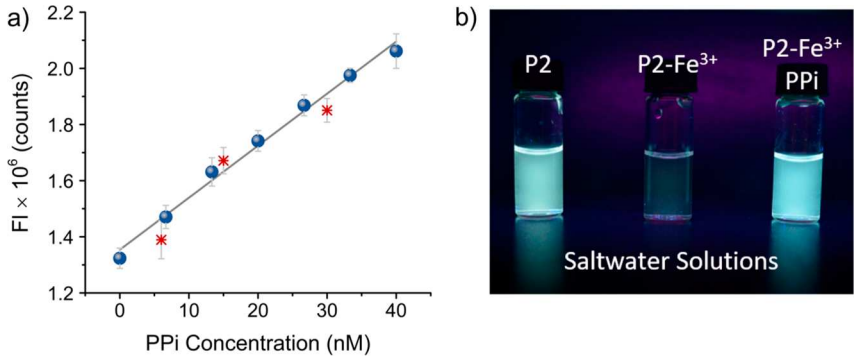

Figure 4. (a) Peak fluorescence intensity of **P2**-Fe^{3+} with respect to PPi concentration (blue spheres) and intensities measured from seawater samples with known amounts of PPi (red stars) (λ_{ex} = 380 nm, λ_{em} = 463 nm). Error bars correspond to standard errors measured from three samples. (b) Picture of **P2** solutions in artificial seawater showing the on−off−on fluorescence behavior upon subsequent additions of Fe^{3+} and PPi.

slope is the Stern−Volmer constant (K_{SV}) (Figure 2c). The plot has a linear range between 0 and 7.3 × 10^{-6} M Fe^{3+} with a K_{SV} of 3.4 × 10^5 M. The strong linearity and high K_{SV} indicate a static and amplified quenching mechanism, respectively, and there is no observable variation in the fluorescence lifetimes of **P2** and **P2**-Fe^{3+}, which further indicates a static quenching mechanism (Figure S7). Above the linear region, the magnitude of the fluorescence response with respect to Fe^{3+} concentration decreases (Figure S6a). The evolution in the absorbance of **P2** upon Fe^{3+} addition is shown in Figure 2f. The absorption maximum (λ_{max}) only slightly blue-shifts 5 nm from 378 to 383 nm, indicating that the binding of Fe^{3+} has little effect on the electronic structure of **P2**. Upon the addition of PPi (up to 5.3 × 10^{-6} M) to **P2**-Fe^{3+}, the quenched fluorescence is almost fully recovered (Figure 2e). We found that the addition of Fe^{3+} to quench the fluorescence to approximately 85% of the maximum was optimal for maximizing the sensitivity of the assay. When **P2** is fully quenched, the initial addition of PPi does not result in immediate fluorescence recovery (Figure S6b), which leads to lower sensitivities. We hypothesized that the incorporation of the ethynyl linker in the polymer backbone would promote planarity and extend the conjugation length to improve assay sensitivity. Indeed, the absorption and emission maxima of **P2** are significantly red-shifted compared to those reported for a CPE with a fluorene-*alt*-phenylene backbone (334 and 411 nm, respectively), and a 2 orders of magnitude enhancement in the sensitivity is observed.[20,27]

To accurately determine PPi concentration in complex aqueous environments, it is important that the on−off−on fluorescent behavior of **P2** is not strongly influenced by cations and anions other than Fe^{3+} and PPi. Therefore, a series of selectivity tests were performed to individually assess the effect of various cations and anions on the fluorescent properties of **P2** and **P2**-Fe^{3+}, respectively. With the intent of utilizing **P2** as a PPi sensor in marine environments, we investigated the effects of Na^+, K^+, Mg^{2+}, Ca^{2+}, and Sr^{2+}, as these are the most prevalent cations in seawater (>1 ppm), as well as a variety of minor cations found in seawater including: Co^{2+}, Fe^{2+}, Mn^{2+}, Ni^{2+}, and Zn^{2+}.[30] Figure 3a plots I_q/I_{oq} − 1, where I_{oq} is the fluorescence intensity of neat **P2** in DI water, and I_q is the intensity of **P2** in the presence of the various cations combined in a 1:100 molar ratio of **P2** to metal cations. Negative values correspond to fluorescence quenching, whereas positive values represent fluorescence enhancement. The presence of Fe^{3+} and Co^{2+} induced the greatest reduction of the emission intensity at 80% and 40%, respectively. Some cations, such as Fe^{2+} and Mn^{2+}, slightly enhanced the fluorescence. In comparison, Fe^{3+} most significantly quenched the fluorescence of **P2**, demonstrating that the fluorescence quenching of **P2** is selective toward Fe^{3+} and that cations present in marine and brackish environments would have a minimal effect of the fluorescent signal of **P2**.

Using a similar analysis, the fluorescence response of **P2**-Fe^{3+} to a variety of anions was also evaluated. Anions ranged from the major anionic constituents in seawater; F^-, Br^-, Cl^-, $H_2BO_3^-$, HCO_3^-, and SO_4^{2-}, trace and minor anionic components in seawater; I^-, $C_2H_3O_2^-$, CO_3^{2-}, and NO_3^-, and other phosphates, $H_2PO_4^-$ and PO_4^{3-}.[30] In these experiments, the fluorescence of **P2** was quenched by 85% with Fe^{3+} and the molar ratio **P2** to anions was adjusted to 1:100. In Figure 3b, I_d/I_{od} − 1 is plotted, where I_{od} is the fluorescence intensity of **P2**-Fe^{3+} (PPi fluorescence quenched to 85% with Fe^{3+}) and I_d is the fluorescence intensity following the addition of the various anions. In the presence of PPi, the fluorescence of **P2**-Fe^{3+} rapidly increases four-fold, whereas, the addition of other phosphate anions, $H_2PO_4^-$ and PO_4^{3-}, only slightly dequenched the fluorescence. The other anions have minimal effect on the emission intensity of **P2**-Fe^{3+} indicating the dequenching behavior of **P2**-Fe^{3+} is highly selective toward PPi and could potentially function as a PPi sensor in more-complex systems.

To demonstrate the potential of **P2** to serve as a PPi sensor in complex aquatic environments, a fluorescence assay was designed to measure PPi concentrations in artificial seawater. A calibration curve of the fluorescence intensity of **P2**-Fe^{3+} with respect to PPi concentration is shown in Figure 4a, with a linear response observed from 0 to 40 nM PPi. The limit of detection (LOD), defined as the lowest concentration of analyte that can be detected, was calculated to be 4 nM using the equation LOD = 3 δ/m, where δ and m are the standard deviation and slope of the calibration line, respectively. Artificial seawater solutions with known amounts of PPi (6, 15, and 30 nM) were prepared with Instant Ocean sea salt. In a typical assay, 3 μL of **P2**-Fe^{3+} (0.2 mM **P2** and 0.1 mM Fe^{3+}) was added to a 3 mL seawater sample, and the fluorescence intensity at 463 nm was measured (λ_{ex} = 380 nm). The averaged results from three trials are plotted in Figure 4a, which demonstrates that the experimental data are in good agreement with the theoretical values. The limit of quantification (LOQ), defined as the lowest concentration of analyte that can be quantified, was determined using a

DOI: 10.1021/acsapm.8b00064
ACS Appl. Polym. Mater. 2019, 1, 309−314

precision profile approach to account for any potential variability in the fluorescence measurements due to the presence of cations and anions in the artificial seawater. The LOQ was found to be 6 nM within a 10% relative standard deviation, demonstrating the ability of **P2** to accurately measure PPi in a complex environment at parts-per-billion concentrations. This system demonstrates one of the lowest detection limits of solution-based conjugated polymer systems for the detection of PPi in aqueous systems while also operating in a marine environment (Table S1).[17,19,20,22,23]

In conclusion, we demonstrate a facile on−off−on fluorescent assay for PPi detection in complex aqueous environments. A rigid water-soluble CPE with a poly(fluorene-*co*-ethynyl) backbone and sulfate functionalized side-chains was rationally designed to incorporate selective analyte−receptor interactions and promote enhanced signal amplification. The target CPE was rapidly synthesized using a straightforward approach employing a microwave-assisted Stille cross-coupling polymerization and thiol−ene click chemistry post-polymerization modification. This broadly applicable method enables facile access to the reported system **P2** and other CPEs with an overall reduction in synthetic steps and purification procedures. It was shown that the polymer fluorescence is selectively quenched by Fe^{3+} through an amplified and static quenching mechanism, and upon subsequent addition of PPi, the fluorescence is almost completely restored at concentrations as low as 5.3×10^{-6} M. Accurate detection of PPi in complex and challenging aqueous environments was evaluated using artificial seawater samples with known amounts of PPi, and the LOD and LOQ were found to be 4 and 6 nM PPi, respectively. The performance of this assay offers promising opportunities for also monitoring PPi in biological aquatic ecosystems, while the broad utility of thiol−ene click chemistry offers the potential for the straightforward integration of other diverse sensing elements.

■ ASSOCIATED CONTENT

Supporting Information

The Supporting Information is available free of charge on the ACS Publications website at DOI: 10.1021/acsapm.8b00064.

Additional details on experimental methods, synthetic procedures, ^{1}H NMR spectra, additional absorption and fluorescence data, time-resolved fluorescence spectroscopy, and a comparison with other CP sensors (PDF)

■ AUTHOR INFORMATION

Corresponding Author

*E-mail: jason.azoulay@usm.edu.

ORCID

Naresh Eedugurala: 0000-0003-4714-7993

Jason D. Azoulay: 0000-0003-0138-5961

Author Contributions

†A.K.W. and J.T. contributed equally to this work.

Notes

The authors declare no competing financial interest.

■ ACKNOWLEDGMENTS

The work performed was made possible through the support from the National Science Foundation (NSF OIA-1632825). A.K.W. acknowledges support from the NSF Graduate Research Fellowship under grant no. GR05384.

■ REFERENCES

(1) Kim, S. K.; Lee, D. H.; Hong, J.-I.; Yoon, J. Chemosensors for Pyrophosphate. *Acc. Chem. Res.* **2009**, *42*, 23−31.

(2) Nelson, D. L.; Cox, M. M.; Lehninger, A. L. *Lehninger Principles of Biochemistry*; W.H. Freeman: New York, 2013; pp 505−525.

(3) Ronaghi, M.; Karamohamed, S.; Pettersson, B.; Uhlén, M.; Nyrén, P. Real-Time DNA Sequencing Using Detection of Pyrophosphate Release. *Anal. Biochem.* **1996**, *242*, 84−89.

(4) Lee, S.; Yuen, K. K. Y.; Jolliffe, K. A.; Yoon, J. Fluorescent and Colorimetric Chemosensors for Pyrophosphate. *Chem. Soc. Rev.* **2015**, *44*, 1749−1762.

(5) Correll, D. L. The Role of Phosphorus in the Eutrophication of Receiving Waters: A Review. *J. Environ. Qual.* **1998**, *27*, 261−266.

(6) Sundareshwar, P. V.; Morris, J. T.; Pellechia, P. J.; Cohen, H. J.; Porter, D. E.; Jones, B. C. Occurrence and Ecological Implications of Pyrophosphate in Estuaries. *Limnol. Oceanogr.* **2001**, *46*, 1570−1577.

(7) Jolliffe, K. A. Pyrophosphate Recognition and Sensing in Water Using Bis[zinc(II)dipicolylamino]-Functionalized Peptides. *Acc. Chem. Res.* **2017**, *50*, 2254−2263.

(8) Lee, H. N.; Swamy, K. M. K.; Kim, S. K.; Kwon, J.-Y.; Kim, Y.; Kim, S.-J.; Yoon, Y. J.; Yoon, J. Simple but Effective Way to Sense Pyrophosphate and Inorganic Phosphate by Fluorescence Changes. *Org. Lett.* **2007**, *9*, 243−246.

(9) Cho, H. K.; Lee, D. H.; Hong, J.-I. A Fluorescent Pyrophosphate Sensor via Excimer Formation in Water. *Chem. Commun.* **2005**, *0*, 1690−1692.

(10) Lee, H. N.; Xu, Z.; Kim, S. K.; Swamy, K. M. K.; Kim, Y.; Kim, S.-J.; Yoon, J. Pyrophosphate-Selective Fluorescent Chemosensor at Physiological pH: Formation of a Unique Excimer upon Addition of Pyrophosphate. *J. Am. Chem. Soc.* **2007**, *129*, 3828−3829.

(11) Langton, M. J.; Serpell, C. J.; Beer, P. D. Anion Recognition in Water: Recent Advances from a Supramolecular and Macromolecular Perspective. *Angew. Chem., Int. Ed.* **2016**, *55*, 1974−1987.

(12) Hargrove, A. E.; Nieto, S.; Zhang, T.; Sessler, J. L.; Anslyn, E. V. Artificial Receptors for the Recognition of Phosphorylated Molecules. *Chem. Rev.* **2011**, *111*, 6603−6782.

(13) Jiang, H.; Taranekar, P.; Reynolds, J. R.; Schanze, K. S. Conjugated Polyelectrolytes: Synthesis, Photophysics, and Applications. *Angew. Chem., Int. Ed.* **2009**, *48*, 4300−4316.

(14) Thomas, S. W.; Joly, G. D.; Swager, T. M. Chemical Sensors Based on Amplifying Fluorescent Conjugated Polymers. *Chem. Rev.* **2007**, *107*, 1339−1386.

(15) Chen, L.; McBranch, D. W.; Wang, H.-L.; Helgeson, R.; Wudl, F.; Whitten, D. G. Highly Sensitive Biological and Chemical Sensors based on Reversible Fluorescence Quenching in a Conjugated Polymer. *Proc. Natl. Acad. Sci. U. S. A.* **1999**, *96*, 12287−12292.

(16) Lv, F.; Wang, S.; Bazan, G. C. Sensing Applications via Energy Transfer from Conjugated Polyelectrolytes. In *Conjugated Polyelectrolytes*; Wiley-VCH: Weinheim, Germany, 2013; pp 201−229.

(17) Zhu, X.; Yang, J.; Schanze, K. S. Conjugated Polyelectrolytes with Guanidinium Side Groups. Synthesis, Photophysics and Pyrophosphate Sensing. *Photochem. Photobiol. Sci.* **2014**, *13*, 293−300.

(18) Wu, W.; Bazan, G. C.; Liu, B. Conjugated-Polymer-Amplified Sensing, Imaging, and Therapy. *Chem* **2017**, *2*, 760−790.

(19) Zhao, X.; Liu, Y.; Schanze, K. S. A Conjugated Polyelectrolyte-based Fluorescence Sensor for Pyrophosphate. *Chem. Commun.* **2007**, *0*, 2914−2916.

(20) Dwivedi, A. K.; Saikia, G.; Iyer, P. K. Aqueous Polyfluorene Probe for the Detection and Estimation of Fe^{3+} and Inorganic Phosphate in Blood Serum. *J. Mater. Chem.* **2011**, *21*, 2502−2507.

(21) Pu, K.-Y.; Wang, G.; Liu, B. Design and Synthesis of Conjugated Polyelectrolytes. In *Conjugated Polyelectrolytes*; Wiley-VCH: Weinheim, Germany, 2013; pp 1−64.

(22) Li, Z.; Acharya, R.; Wang, S.; Schanze, K. S. Photophysics and Phosphate Fluorescence Sensing by Poly(phenylene ethynylene)

DOI: 10.1021/acsapm.8b00064
ACS Appl. Polym. Mater. 2019, 1, 309−314

Conjugated Polyelectrolytes with Branched Ammonium Side Groups. *J. Mater. Chem. C* **2018**, *6*, 3722−3730.
(23) Zhao, X.; Schanze, K. S. Fluorescent Ratiometric Sensing of Pyrophosphate via Induced Aggregation of a Conjugated Polyelectrolyte. *Chem. Commun.* **2010**, *46*, 6075−6077.
(24) Chen, Z.; Wu, P.; Cong, R.; Xu, N.; Tan, Y.; Tan, C.; Jiang, Y. Sensitive Conjugated-Polymer-Based Fluorescent ATP Probes and Their Application in Cell Imaging. *ACS Appl. Mater. Interfaces* **2016**, *8*, 3567−3574.
(25) Hoyle, C. E.; Bowman, C. N. Thiol−Ene Click Chemistry. *Angew. Chem., Int. Ed.* **2010**, *49*, 1540−1573.
(26) Wei, B.; Ouyang, L.; Liu, J.; Martin, D. C. Post-Polymerization Functionalization of Poly(3,4-propylenedioxythiophene) (PProDOT) via Thiol−Ene "Click" Chemistry. *J. Mater. Chem. B* **2015**, *3*, 5028−5034.
(27) Vonnegut, C. L.; Tresca, B. W.; Johnson, D. W.; Haley, M. M. Ion and Molecular Recognition Using Aryl−Ethynyl Scaffolding. *Chem. Asian J.* **2015**, *10*, 522−535.
(28) London, A. E.; Huang, L.; Zhang, B. A.; Oviedo, M. B.; Tropp, J.; Yao, W.; Wu, Z.; Wong, B. M.; Ng, T. N.; Azoulay, J. D. Donor−Acceptor Polymers with Tunable Infrared Photoresponse. *Polym. Chem.* **2017**, *8*, 2922−2930.
(29) Liu, Y.; Ogawa, K.; Schanze, K. S. Conjugated Polyelectrolyte Based Real-Time Fluorescence Assay for Phospholipase C. *Anal. Chem.* **2008**, *80*, 150−158.
(30) Atkinson, M.; Bingman, C. Elemental Composition of Commercial Seasalts. *J. Aquaricult. Aquat. Sci.* **1997**, *8*, 39−43.

DOI: 10.1021/acsapm.8b00064
ACS Appl. Polym. Mater. 2019, 1, 309−314